An in-depth four-year investigation into corrosion of carbon steel materials in the secondary cooling piping of the 30 MW RSG GAS research reactor

G.R. Sunaryo,[1]* M.I. Santoso,[2] R. Kusumastuti,[3] D.S. Wisnubroto[4] and Sriyono[1]

[1]*Research and Technology Center for Nuclear Reactor, Research Organization for Nuclear Energy, ORTN-BRIN, South Tangerang, Indonesia*
[2]*Sekolah Tinggi Teknik Nuklir, Yogyakarta, Indonesia*
[3]*Research Organization for Nanotechnology and Material, ORNM-BRIN, South Tangerang, Indonesia*
[4]*Research and Technology Center for Radioactive Waste and Fuel Cycle Research Center,ORTN-BRIN, South Tangerang, Indonesia*
**E-mail: geni001@brin.go.id; genirs@yahoo.com*

Abstract

An observational study examined carbon steel's performance in PUSPIPTEK tap water, used as raw water for the RSG GAS secondary cooling system. Disc-shaped coupons (5 cm diameter) categorized into three series explored uniform, galvanic, and crevice corrosion processes using carbon steel and Stainless Steel 304. Coupons were immersed continuously for four years in a flow-controlled holding pond. Various methods for observing the water quality and material surface, including visual photography, microscopy, and X-ray diffractometry (XRD), were employed. Analysis revealed sulfate and calcium ions within Safety Analysis Report (SAR) limits for secondary cooling water, while chloride ions and water hardness exceeded allowable levels. pH and water conductivity remained acceptable. Carbon steel exhibited a corrosion rate of $1.19 \cdot 10^{-4}$ m per year. Visual inspection showed diverse corrosion product colors, while microscopy revealed distinct surface degradation, especially pitting. XRD detected compounds, such as $FeCl_3$, Fe_3O_4, $Fe_2(SO_4)_3$, Fe_2O_3, $FeSO_4$, $FeCl_2$, FeS, $Fe(OH)_3$, and FeO, indicating oxidation-reduction reactions. The corrosion process was sustained due to extended immersion and altered the metal surface structure, particularly at grain boundaries. Pitting corrosion occurred in crevices and galvanic circuits, with the uniform coupon circuit severely corroded. This underscores the necessity for corrosion inhibitors in RSG GAS secondary cooling water systems.

Received: November 30, 2023. Published: May 8, 2024 doi: 10.17675/2305-6894-2024-13-2-11

Keywords: *corrosion, PUSPIPTEK water, carbon steel, surveillance corrosion, RSG-GAS 30MW.*

Introduction

The corrosion of carbon steel (CS) within the water environment at PUSPIPTEK constitutes a critical concern requiring comprehensive understanding, particularly as an initial investigation, with a focus on aging management [1]. This water serves a dual purpose, serving as both the secondary cooling fluid for the Nuclear Research Reactor GA Siwabessy (RSG-GAS) 30MW and as the raw water source for producing demineralized water used in the primary cooling fluid [2]. Moreover, CS serves as the primary material for constructing secondary cooling pipes. Consequently, the urgency of ensuring material reliability is underscored, particularly when considering reactor operation safety aspects [3–6]. The occurrence of a pipe leak may trigger suboptimal heat recovery within the primary cooling system, resulting in a diminished safety level of reactor operation [7–9]. This issue is especially undesirable for the 30MW RSG-GAS situated in Serpong, Indonesia, and operational since 1986 [10]. The research reactor comprises key components supporting the reactor material structure, including tanks, fuel cladding, heat exchangers, as well as primary and secondary cooling systems [11, 12].

Furthermore, corrosion incidents, particularly pittings, are economically significant not only in nuclear facilities but also in oil and gas installations exposed to CO_2/H_2S-saturated brines [13–16]. Physical parameters such as temperature and environmental conditions like pH and chlorine ion concentration exert strong influences on the pitting process [17–22]. Addressing these challenges is imperative for enhancing safety and economic efficiency in various industrial contexts.

The management of cooling water quality is a crucial aspect in guaranteeing the safe functionality of the reactor, as it significantly influences the operational lifespan [23]. Enhanced oversight of cooling water quality directly correlates to improved material reliability, which in turn contributes to the extension of the reactor's operational life. In this context, the specifications for elemental content in primary cooling water are rigorously defined and mandated in the Safety Analysis Report (SAR), necessitating strict compliance. Furthermore, it is imperative to regularly submit the results of chemical analyses of the water to the regulatory authority, Badan Pengawas Tenaga Nuklir (BAPETEN), as part of ongoing monitoring and regulatory requirements.

The impact of reactor cooling water quality control on structural materials can be effectively monitored through the implementation of corrosion control using coupons [12, 24]. Inadequate water quality can lead to heightened corrosion levels and the formation of deposits (scale). If such issues arise in the fuel cladding and reactor tank, there exists the potential for the release of radioactive materials into the environment, posing risks to personnel.

Assessing material corrosion resistance involves considering various facets, including metallurgical, electrochemical, physical, and chemical aspects, as well as thermodynamic considerations. The electrochemical aspect involves wet corrosion processes due to the presence of an electrolyte, in contrast to dry corrosion processes devoid of electrolyte. Since

primary and secondary cooling water functions as an electrolyte, the wet corrosion process assumes a crucial role in RSG-GAS.

Wet corrosion, being an electrochemical process, arises from potential differences between two metal surfaces, where the lower potential undergoes oxidation. The corrosion rate is notably influenced by temperature, with higher electrolyte temperatures resulting in increased corrosion rates [25]. This phenomenon is evident in the supporting material for the RSG GAS secondary cooling system, operating at approximately 40°C and affected by debris entry from the open-air environment in the cooling tower (CT), a key parameter driving the corrosion process.

The raw water utilized originates from PUSPIPTEK water management and possesses a high mineral content, notably including chlorine with chlorite for bacterial eradication. Consequently, there exists a significant potential for initiating the corrosion process and the formation of surface scale on materials. Mitigating measures, such as the addition of corrosion inhibitors, anti-scaling agents, and antimicrobial substances, are prescribed solutions documented in the Safety Analysis Report (SAR). However, understanding the optimal concentration and potential corrosion impact within the PUSPIPTEK aqueous environment necessitates further investigation, thus motivating the need for dedicated research efforts.

Initiatives related to corrosion control were initiated as early as 2007, with visual observation results after a 3-month immersion process in the PUSPIPTEK water environment being presented at various international forums and national journals [2, 26, 27]. However, a comprehensive metallurgical analysis after a 4-year immersion process is addressed in this paper.

The primary objective of this research is to scrutinize the corrosion behavior of carbon steel (CS) exposed to PUSPIPTEK water, emphasizing metallurgical changes. This study serves as a reference for subsequent investigations aimed at comprehending the mechanism and effectiveness of incorporating inhibitors at concentrations recommended by the Safety Analyses Report (SAR). The CS material is configured in disc form with a 5 cm diameter, aligning with the availability of a large cross-sectional area of the raw material. The coupons are strategically arranged to obtain uniform, crevice, and galvanic corrosion data. To observe galvanic corrosion from CS, a companion material, CS-304 with a 15 cm diameter, was employed. A detailed design akin to corrosion coupons, previously executed for assessing RSG GAS primary cooling water quality, is elaborated in prior publications [28, 29]. Metallographic observations are conducted through microscopy and X-ray Diffractometry (XRD), while chemical water analysis employs the UV-Vis Spectrophotometry method.

Methodology

Coupon series design

In this investigation, corrosion observations were carried out utilizing a coupon rack designed as depicted in Figure 1. The coupon rack was systematically arranged both

vertically and horizontally, submerging it in the feedwater of PUSPIPTEK RSG GAS. The utilization of the coupon rack facilitated a comprehensive examination of diverse corrosion types, encompassing galvanic and uniform corrosion phenomena.

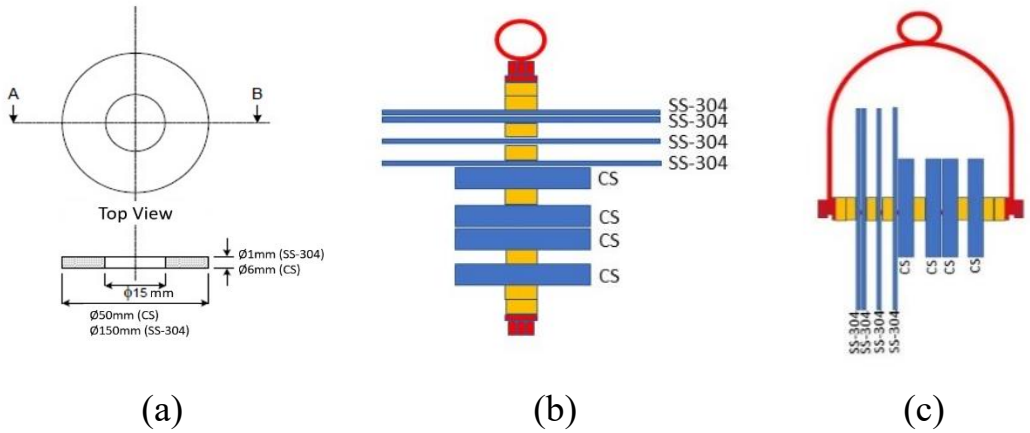

(a) (b) (c)

Figure 1. The design of a series of corrosion control coupons within the PUSPIPTEK water tank, featuring (a) coupon size, (b) horizontal series, and (c) vertical series.

Analysis of coupons

The study employed X-ray Fluorescence (XRF) analysis to determine the elemental composition of carbon steel (CS). This non-destructive technique uses X-rays to excite the atoms in the sample, causing them to emit secondary (fluorescent) X-rays. By analyzing these emitted X-rays, one can identify and quantify the elements present in the material. The data obtained from the XRF analysis is crucial as it provides a baseline for understanding how the composition of CS changes after being submerged in PUSPIPTEK water for four years.

Following the outlined immersion procedure shown in Figure 2, the coupons were submerged for this duration. Post-immersion, the coupons were retrieved for detailed examination. A comprehensive visual inspection was first conducted using photography to document any observable surface changes, providing an initial qualitative assessment of the corrosion effects.

For a more in-depth analysis, the coupons underwent corrosion depth profiling through microscopic analysis. This involved the vertical sectioning of specific areas of the coupons, embedding them in epoxy to stabilize the samples for further processing. The samples were then subjected to a series of preparatory steps – mounting, grinding, polishing, and etching, which are standard metallurgical procedures to prepare a sample for microscopic examination. This meticulous process allows for a detailed investigation of the corrosion effects, revealing changes in the material structure and providing insights into different types of corrosion, such as uniform, crevice, galvanic, and particularly pitting corrosion.

Furthermore, the identification of corrosion product compounds was conducted using X-ray diffraction (XRD) analysis. In this technique, X-rays are directed at the material, and the way these rays are scattered by the sample provides information about the

crystallographic structure of the compounds present. Samples for XRD were taken from various depths of the corroded layer, from the outer surface to the inner regions of the coupons, ensuring a thorough representation of the corrosion products. The XRD results were then compared with standard reference patterns from the Joint Committee of Powder Diffraction Standards (JCPDS) using the PCPDFWIN program. This comparison allowed for the accurate identification of specific compounds formed during the corrosion process, contributing significantly to the understanding of the chemical nature of the corrosion products.

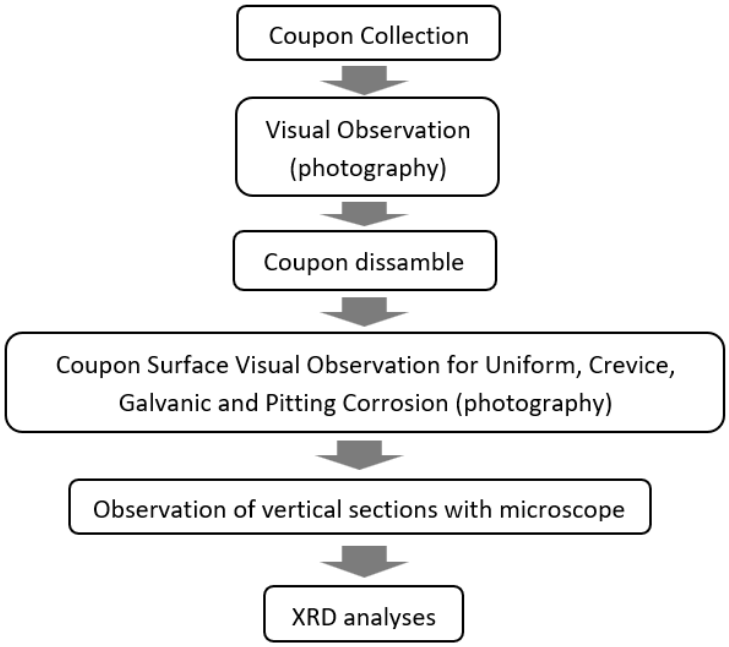

Figure 2. A step-by-step coupon immersion procedure in adherence to outlined protocols.

Water chemistry analysis

In the study, water samples were meticulously collected from three specific locations within the PUSPIPTEK water holding pond, as detailed in Figure 3. These sampling sites were strategically chosen where corrosion coupons had been submerged for a prolonged period of four years, immersed to about half the depth of the water body. To ensure the reliability and accuracy of the analytical results, each water sample was subjected to triplicate measurements. This practice is a standard scientific approach to minimize errors and variations, thereby enhancing the robustness of the data.

The pH levels of the water samples, an indicator of the acidity or alkalinity, were accurately determined using a pH-meter. This measurement is crucial as pH is a key factor that can influence the corrosion behavior of materials. The concentrations of various ions in the water, including sulfate, phosphate, chloride, ferrous, and zinc, were quantified using Ultraviolet-Visible (UV-Vis) spectrophotometry. This technique involves measuring the

absorption of light at specific wavelengths, which is a reliable method for determining the concentration of these ions in the water.

Additionally, the analysis of calcium ions was conducted through a titration method using a standard solution of potassium hydroxide. Titration is a common laboratory method of quantitative chemical analysis used to determine the concentration of an identified analyte. In this case, it helped in assessing the amount of calcium present in the water samples.

The total hardness of the water, which is primarily a measure of the concentration of calcium and magnesium ions, was also evaluated through titration. This process employed a buffer solution and Ethylenediaminetetraacetic acid (EDTA), a chelating agent. The determination of total hardness was based on a noticeable color change from pink to blue during the titration process. Hardness is a critical parameter in water quality analysis, especially in the context of corrosion, as it can significantly impact the rate and nature of corrosion in various metals.

These comprehensive and scientifically rigorous analytical methods provided a detailed chemical profile of the water, which is essential for understanding the corrosion environment in the PUSPIPTEK water holding pond and for evaluating the long-term effects of this environment on different materials.

Corrosion rate analysis

In this study, the corrosion rate of carbon steel (CS) was accurately measured using the potentiostat method with a GAMRY instrument. This method involves applying a controlled potential to the CS sample and measuring the resulting current, which provides information about the corrosion rate. This technique is widely recognized for its precision in evaluating corrosion rates in various environments.

To quantify the extent of corrosion, the study utilized a specific formula [30]:

$$w = Cr \cdot t \cdot A \cdot \rho \tag{1}$$

where w represents the weight loss (kg), Cr denotes the corrosion rate (mm per year), t signifies the immersion time (years), A represents the sample area (m^2), ρ is the material density ($kg \cdot m^{-3}$).

This formula is critical in estimating the weight loss of carbon steel (CS) due to corrosion in PUSPIPTEK water. Accurate corrosion rate measurements are essential to assess CS's resilience in such environments. Understanding corrosion rates is key for various reasons: it informs the correct dosage of corrosion inhibitors, protecting CS pipes; it aids in preventing leaks, reducing the risk of severe incidents; and it helps develop maintenance plans that are both effective and cost-effective, aimed at preventing failures and extending the infrastructure's lifespan.

In conclusion, using the potentiostat method with GAMRY for measuring CS's corrosion rate in specific environments, coupled with this formula, provides an effective

means to gauge material degradation over time. Such information is vital to maintain the safety, reliability, and economic viability of systems and structures utilizing Carbon Steel.

Results and Discussion

Water analysis

A comprehensive analysis of the chemical composition of PUSPIPTEK water, in comparison to the established limits for RSG GAS secondary water, is presented in Table 1. A meticulous examination of Table 1 reveals that the sulfate ion content falls below the limit stipulated in the Safety Analysis Report (SAR), while the hardness slightly exceeds the prescribed threshold. The calcium content is approximately at the specified threshold, whereas chloride ions are nearly twice the permissible limit, potentially posing a risk of inducing pitting corrosion. This observation aligns with previous findings [31, 32]. The acidity level remains within the neutral pH range, as does the conductivity.

Table 1. Chemical composition analysis of PUSPIPTEK water.

Parameter	PUSPIPTEK water	RSG GAS secondary cooling water limit value Safety Analyses Report (SAR)
SO_4 (sulphate)/ppm	51.44±1.89	67.8
Hardness Total/ppm	46.33±1.67	40
Ca/ppm	34.67±1.33	34
Cl^-/ppm	13±2.0	7.1
pH	7.41±0.31	7~7.5
Temperature/°C	27.33±0.07	–
Conductivity/(S/cm)	149.92±0.64	150

Composition analysis of CS material

To evaluate the surface condition of CS after a 4-year immersion in PUSPIPTEK water, a scanning electron microscopy (SEM) analysis was performed using the ZAF method. The results of the SEM examination are presented in Figure 3, while the chemical elemental composition of CS, analyzed by XRF, is elaborated in Table 2.

Table 2. Chemical elemental composition of carbon steel (CS) following a 4-year immersion in PUSPIPTEK water, analyzed by XRF.

Element	SEM	XRF
Fe	98.06±0.21	99.42±0.001
Si	0.28±0.27	0.30±0.05
Al	0.61±0.31	–

Element	SEM	XRF
C	1.06±0.21	–
Mn	–	0.30±0.17
Ti	–	0.05±0.01

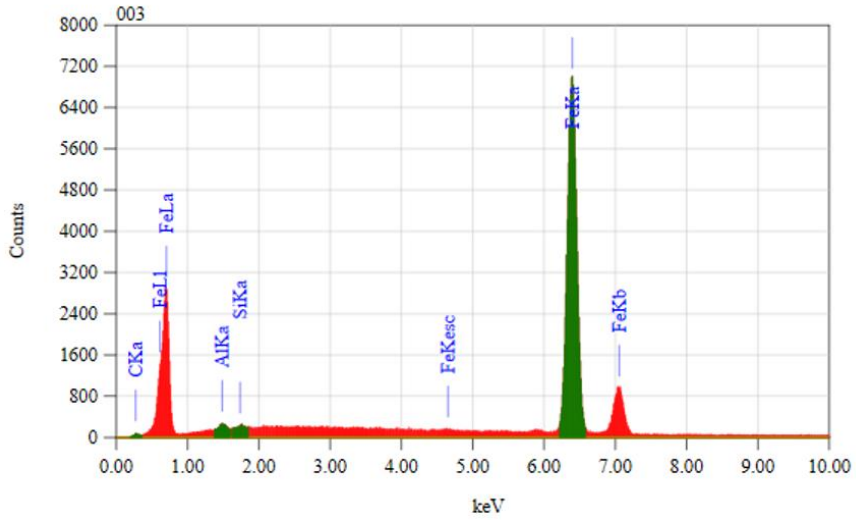

Figure 3. Surface evaluation of carbon steel (CS) after 4-year immersion in PUSPIPTEK Water using SEM-ZAF analysis.

Visual inspection of coupon surfaces

The results of the visual examination of coupons immersed in the PUSPIPTEK water environment are illustrated in Figures 4 and 5.

The analysis of Figure 4 reveals a notable increase in the thickness of corrosion products on carbon steel (CS) chips after a 4-year immersion period (Figure 4(b)) compared to the observations made at the 4-month mark (Figure 4(a)). This finding implies a direct correlation between prolonged immersion time and the intensified thickness of corrosion products.

The observed increase in thickness can be attributed to the continuous exposure of CS to the aqueous environment, leading to a progressive accumulation of corrosion by-products. During this prolonged exposure, various electrochemical reactions occur at the CS surface, resulting in the formation and deposition of corrosion products.

Figure 5 offers a comprehensive comparative assessment of visual observations between the horizontal and vertical series. In both configurations, corrosion products conspicuously accumulate on CS plates, uniformly covering the entire surface, exhibiting characteristics indicative of uniform, crevice, or galvanic corrosion. The compounds formed display a spectrum of colors, ranging from yellow, orange, red to nearly black, suggesting the presence of different oxidation states and compounds in the corrosion products.

(a) (b)

Figure 4. Visual examination results of coupons immersed in PUSPIPTEK water tank – vertical series. (a) 4 Months of immersion [25]; (b) 4 years of immersion.

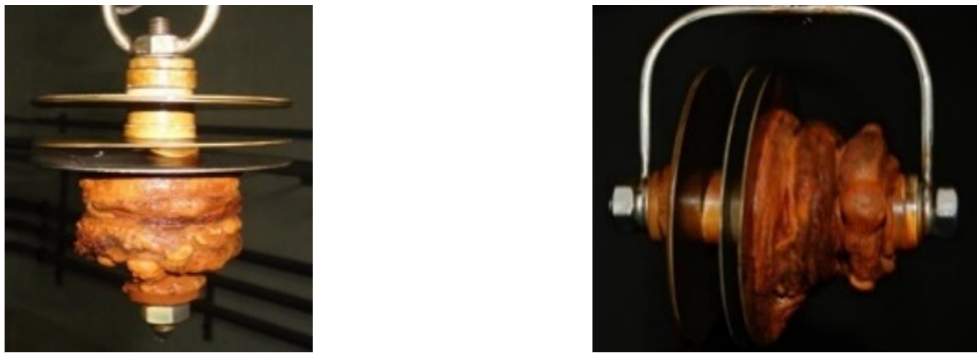

(a) (b)

Figure 5. Visual inspection results of coupons after 4 years of immersion in PUSPIPTEK water tank. (a) Horizontal coupon series, (b) vertical coupon series.

In contrast, the SS-304 chip exhibits no observable corrosion products; instead, it manifests the effects of splashes from the carbon steel corrosion products. This lack of corrosion on SS-304 indicates its enhanced corrosion resistance in comparison to CS, underscoring the material differences in their responses to the corrosive environment. The protective oxide layer formed on the surface of SS-304 contributes to its resistance against corrosion, highlighting the material's superior performance under prolonged exposure to the aggressive aqueous environment.

The visual alterations on the CS surface, observed from both horizontal and vertical orientations for the purpose of studying uniform corrosion, are presented in Figure 6. It is evident that the immersion position, whether horizontal or vertical, does not exhibit any significant differences after 4 years of immersion.

This lack of notable differences in visual alterations implies that the uniform corrosion experienced by the CS surface is relatively consistent regardless of its orientation during the 4-year immersion period. The consistent appearance from both horizontal and vertical perspectives suggests a uniform distribution of the corrosion process across the entire CS

surface, emphasizing the material's susceptibility to uniform corrosion under the specified immersion conditions.

(a) (b) (c)

Figure 6. Visual changes on the surface of carbon steel for uniform corrosion observation after 4 years of immersion in the PUSPIPTEK water tank. (a) Before immersion, (b) horizontal immersion, (c) vertical immersion.

Galvanic corrosion between CS and SS-304 is shown in Figure 7. This figure effectively demonstrates the electrochemical interactions occurring between these two materials when they are in a galvanic relationship. The arrangement, as depicted both horizontally (see Figure 7b) and vertically (see Figure 7c), highlights the increased propensity of CS to undergo corrosion in contrast to the more inert behavior exhibited by SS-304. This contrast underscores the differential corrosion responses of these materials when exposed to similar conditions, providing valuable insights for material selection and corrosion prevention strategies.

In the galvanic coupling, CS serves as the anodic material, being more reactive, while SS-304 acts as the cathodic material, exhibiting less reactivity. This electrochemical pairing prompts the preferential corrosion of CS in the presence of SS-304. The observed yellow-orange color effect on the SS-304 surface is a visual indication of corrosion by-products from CS adhering to it. It is crucial to recognize that this discoloration is a surface phenomenon rather than inherent corrosion on SS-304.

A noteworthy aspect is the subsequent restoration of the SS-304 surface to its pristine state after brushing. This cleaning process emphasizes the absence of intrinsic corrosion on SS-304, as it efficiently removes the adhered CS corrosion by-products. This phenomenon accentuates the superior corrosion resistance of SS-304 under galvanic conditions and highlights its ability to resist the corrosive effects induced by the more reactive CS.

In summary, the observed galvanic corrosion not only illustrates the electrochemical nature of the corrosion process but also substantiates SS-304's remarkable resistance to corrosion when coupled with the more reactive CS. The ease with which SS-304 sheds the adhered corrosion by-products further underscores its advantageous corrosion-resistant properties in galvanic scenarios.

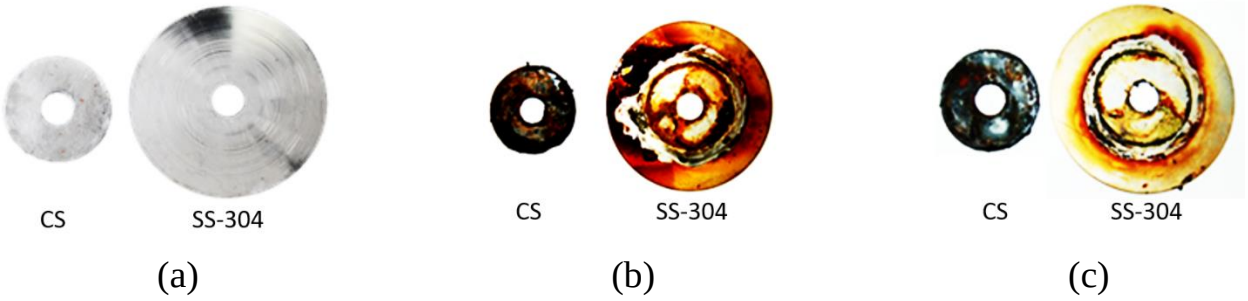

Figure 7. Galvanic corrosion effects on overlapping parts of carbon steel (CS) in series with SS-304 after 4 years of immersion in PUSPIPTEK water. (a) Original sample, (b) horizontal arrangement, (c) vertical arrangement. Insights into electrochemical interactions and corrosion resistance.

Corrosion rate and weight loss analysis

The experimental assessment of the corrosion rate for CS in PUSPIPTEK water conditions yielded a value of $(1.19 \cdot 10^{-4})$ m·per·year. This corrosion rate serves as a quantitative measure of the material loss experienced by carbon steel over the specified time frame, indicating the extent of corrosion per unit area.

To elucidate the practical implications of this corrosion rate, the weight loss of carbon steel was calculated for a 1 cm^3 volume after 4 years of immersion in PUSPIPTEK raw water. Adopting the density of carbon steel as approximately 7.859008 kg/m^3, the estimated weight loss is calculated to be approximately 0.24 kg. This calculated weight loss provides a tangible representation of the material degradation endured by carbon steel during the specified immersion period.

This analysis underscores the significance of the corrosion rate value in evaluating the long-term durability and structural integrity of the material within the given environmental conditions. The calculated weight loss serves as a valuable metric for assessing the real-world consequences of corrosion, emphasizing the importance of monitoring and mitigating corrosion effects to ensure the sustained performance and reliability of carbon steel components in practical applications.

Observation of CS corrosion profile through microscopic analysis

In-depth investigations into the corrosion profile of CS were conducted, incorporating microscopic observations to enhance our understanding of the corrosion characteristics. To achieve this, samples from each series were meticulously vertically sectioned using a manual saw, allowing for a detailed examination of the internal structure.

To ensure stability during microscopic observations, the sectioned CS samples were further embedded in epoxy. This procedure not only secured the samples in a stable matrix but also enhanced the clarity of microstructural features, providing a comprehensive insight into the microscopic corrosion patterns and mechanisms.

The images depicted in Figure 8 provide a detailed visual representation of the microscopic complexities inherent in the corrosion profile of CS. These observations are crucial for a comprehensive understanding of the corrosion mechanism, shedding light on factors such as the distribution of corrosion products, the extent of localized damage, and the potential for variations in corrosion patterns when observed from different orientations. This visual evidence plays a key role in elucidating the intricate aspects of the corrosion process in CS.

The integration of macroscopic and microscopic analyses in this comprehensive approach offers a multi-dimensional understanding of the corrosion behavior of carbon steel under the specified conditions. These observations play a crucial role in refining our comprehension of corrosion mechanisms, facilitating the formulation of effective strategies for corrosion prevention and mitigation in practical applications. Such nuanced insights significantly contribute to advancing the field of corrosion science and engineering, ultimately reinforcing the durability and reliability of materials in diverse industrial settings.

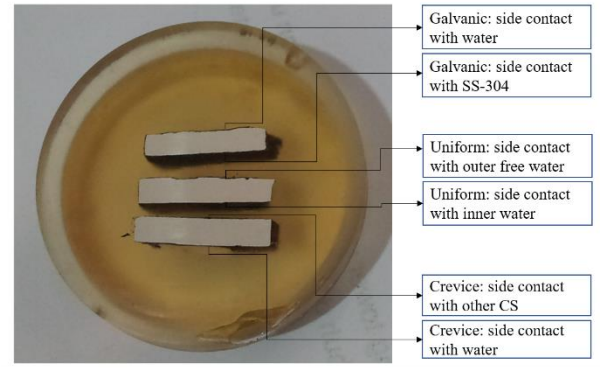

Figure 8. In-depth microscopic analysis of carbon steel (CS) corrosion profile, encompassing galvanic, uniform, and crevice circuits, in vertically sectioned samples embedded in epoxy.

The results of microscopic observations on vertically sectioned samples from the uniform series of CS are presented in Figure 9. This figure provides a visual representation and detailed elucidation of the macrostructural profile of the developed corrosion type. The unit scale indicated in the drawings is 50 μm, allowing for a precise examination of the corrosion features at a microscopic level. This analysis aids in understanding the nature and extent of the corrosion process, contributing valuable insights to the overall study of material degradation in the specified environment.

The corrosion profiles formed on carbon steel metal for the Galvanic and Crevice set coupons are clearly visible. Both Galvanic (Figure 9(a left)) and Crevice (Figure 9(b left)) configurations exhibit pitting corrosion. A distinct image of pitting corrosion with varying depths is presented in Figure 9 c. This occurrence has been extensively discussed in the existing literature, with prior studies addressing the influence of environmental factors on corrosion behavior [32, 33]. The manifestation of pitting corrosion, as observed in Figure 9 c, is a complex phenomenon influenced by multiple factors. Prior research has

established that chloride ions, present in the water, play a predominant role in inducing pitting corrosion in carbon steel [31]. The corrosive nature of chloride ions triggers localized breakdowns in the passive film on the metal surface, initiating the formation of pits. The varying depths of these pits, as evidenced in the microscopic images, further underscore the heterogeneity and severity of the corrosion process.

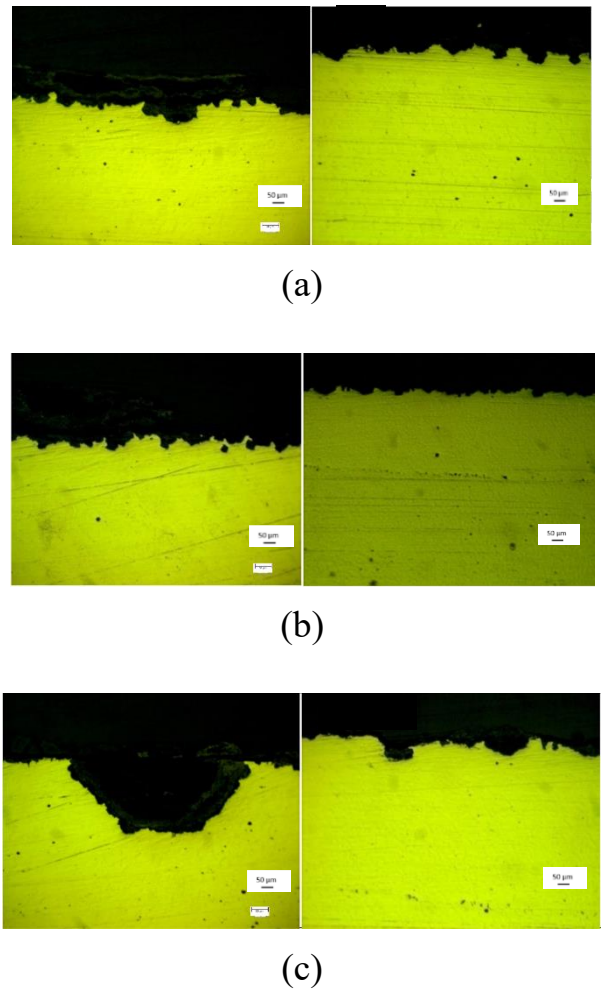

Figure 9. Macrostructural profiling of CS following 4 years of immersion in PUSPIPTEK water, a raw water source for RSG GAS secondary cooling. (a) Galvanic corrosion – left: side contact with water, right: side contact with SS-304; (b) crevice corrosion - left: side contact with other CS, right: side contact with water; (c) pitting resulting from both crevice and galvanic corrosion.

This observed pitting corrosion aligns with the well-documented susceptibility of carbon steel to chloride-induced corrosion in aqueous environments. The discussion within the literature, coupled with the visual evidence from Figure 9, strengthens the understanding of the corrosion mechanisms at play during the 4-year immersion period. The integration of theoretical insights with practical observations contributes to the broader comprehension of material degradation in similar environments, aiding in the formulation of effective corrosion mitigation strategies for practical applications.

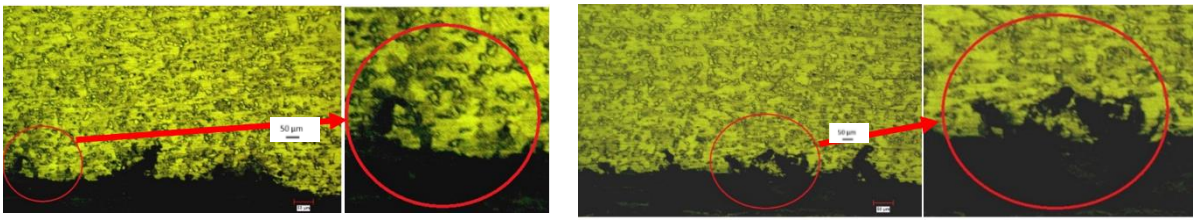

(a) (b)

Figure 10. Intergranular corrosion microstructure profile of carbon steel (CS) after 4 years of immersion in PUSPIPTEK water, a raw water source for RSG GAS secondary cooling water. (a) Crevice circuit, (b) galvanic circuit.

Figure 10 provides a detailed microstructural analysis of carbon steel (CS) using microscopy at a specific magnification. The etching process employed in this observation selectively erodes the grain boundaries, enhancing their visibility. In this micrograph, ferrite is shown in a lighter color, pearlite appears more opaque, and the dark areas represent the passive layer formed by corrosion products.

The corrosion pattern observed is predominantly intergranular, characterized by corrosion predominantly occurring along the grain boundaries. This is often due to the presence of impurities at these boundaries, which are typically introduced during metal manufacturing processes such as precipitation and segregation. These impurities create a distinct layer at the grain boundaries with different physical and chemical properties compared to the bulk metal grains.

The research findings emphasize the vulnerability of CS to grain boundary corrosion, especially in aggressive environments. A notable aspect is the formation of chromium carbides (CrC) at the grain boundaries, which can lead to chromium depletion in adjacent areas. This chromium depletion makes the nearby ferritic matrix more susceptible to corrosion.

Intergranular corrosion is further exacerbated by galvanic reactions. These occur when there is electron transfer between different microstructural features acting as anodic and cathodic sites. This electron transfer leads to the formation of metal ions that react with aggressive ions like hydroxide (OH^-) and chloride (Cl^-) in the environment, known for their corrosive nature. Such reactions weaken the steel's grain lattice, potentially leading to the release of material into the environment, further propagating corrosion and leading to extensive pitting.

This microscopic investigation into the mechanisms of intergranular corrosion provides valuable insights into the material degradation process. It highlights the complex interplay between the environmental conditions, the steel's microstructure, and corrosion kinetics, offering a comprehensive view of the corrosion behavior of carbon steel in specific conditions.

Figure 11 illustrates the severity of the corrosion, showing the maximum depth of pitting corrosion (219.9 μm) and significant surface thinning (330.6 μm) due to uniform

corrosion. Despite these corrosion depths being within safe limits, the study underscores the need for corrosion protection strategies, like the introduction of corrosion inhibitors to PUSPIPTEK water in the RSG GAS secondary cooling system. This measure is crucial for extending the lifespan of the material and aligns with standard practices for corrosion mitigation. It highlights a proactive approach in maintaining the structural integrity and operational safety of materials and components in corrosive environments.

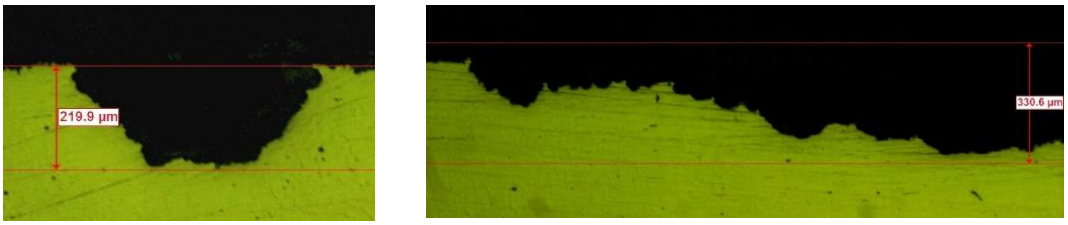

(a) (b)

Figure 11. Examining pitting and uniform corrosion in carbon steel (CS) coupons. (a) Pitting corrosion with a depth of 219.9 µm, (b) uniform corrosion causing surface thinning measured at 330.6 µm.

Corrosion mechanism

The metal coupons and corrosion product compounds from carbon steel (CS) were analyzed using the X-Ray Diffraction (XRD) method. Figure 12 illustrates the analysis results, offering valuable insights into the composition and nature of the corrosion products developed during the immersion period. The XRD analysis helps in understanding the corrosion mechanisms, contributing to a thorough evaluation of CS's corrosion behavior in the specified environment.

A comprehensive examination of the data presented in Figure 12 reveals the presence of various corrosion product compounds on five distinct surfaces: (a) metal CS uniform circuit, (b) under crevice circuit, (c) under galvanic circuit, (d) inner corrosion product, and (e) outer corrosion products. These compounds encompass $FeCl_3$, Fe_3O_4, $Fe_2(SO_4)_3$, Fe_2O_3, $FeSO_4$, $FeCl_2$, FeS, $Fe(OH)_3$, and FeO.

This group of substances clearly shows how the metal element, iron (Fe), interacts with sulfate ions $\left(SO_4^{2-}\right)$, chloride ions (Cl^-), and oxygen from the water. Among these ions, chloride ions, as shown in Table 1) are known to be highly corrosive and are found in high concentrations. The variations in the appearance of small peaks on the XRD curve indicate the presence of other substances in very small amounts, known as trace and noise phases.

While these compounds share similarities in type, differences in intensity values at 2 theta (2θ) angles indicate varying levels of intensity. Some compounds exhibit small yet robust peaks, possibly attributed to unstable crystal formation akin to background noise.

When iron (Fe) reacts with oxygen (O_2) and water (H_2O) in a corrosion process, it doesn't produce just one type of iron oxide compound. Instead, multiple compounds like

FeO, Fe_2O_3, Fe_3O_4, and $Fe(OH)_3$ are formed as a result. The specific compounds that form depend on the pH of the solution and the amount of oxygen present.

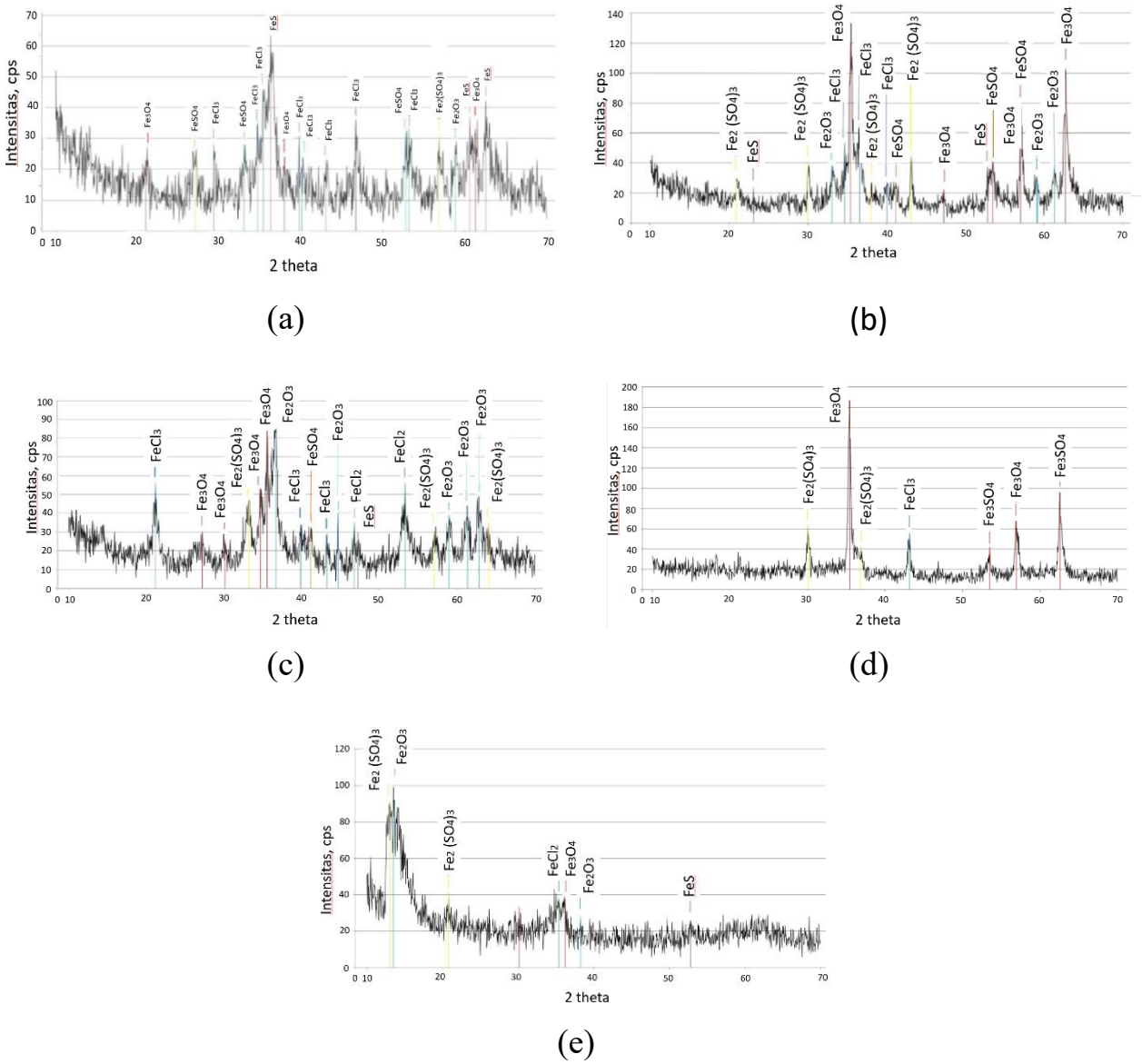

Figure 12. XRD analysis of corrosion product layer on CS coupon after 4 years in PUSPIPTEK raw water pool. (a) Metal CS uniform circuit; (b) under crevice circuit; (c) under galvanic circuit; (d) inner corrosion product; (e) outer corrosion products.

The proposed corrosion reactions of iron (Fe) in the PUSPIPTEK water, influenced by oxygen (O_2) and water (H_2O), depend on factors like the pH and oxygen concentration of the solution. These conditions lead to the formation of various iron oxide compounds. Additionally, the presence of sulfate and chloride ions in PUSPIPTEK water significantly contributes to creating iron chloride and iron sulfate products. Table 3 outlines a theoretical framework of reactions (1)–(15) [30, 35–37], mapping the transition from Fe(II) to the nine identified corrosion products. However, these theoretically suggested reactions require

empirical evidence to confirm their actual occurrence and relevance under the specific conditions of PUSPIPTEK water. This empirical validation is essential, as it will not only confirm but may also adjust the theoretical assumptions, thus improving our understanding of the corrosion processes involved.

Table 3. List of possible reactions leading to the formation of $FeCl_3$, Fe_3O_4, $Fe_2(SO_4)_3$, Fe_2O_3, $FeSO_4$, $FeCl_2$, FeS, $Fe(OH)_3$, and FeO.

No	Reactions
1.	$2Fe(s)+O_2(g)+2H_2O(l)\rightarrow 2Fe(OH)_2(s)$
2.	$Fe(OH)_2(s)\rightarrow \mathbf{FeO}(s)+H_2O(l)$
3.	$4Fe(s)+3O_2(g)+6H_2O(l)\rightarrow 4\mathbf{Fe(OH)_3}(s)$
4.	$4Fe(OH)_3(s)\rightarrow 2\mathbf{Fe_2O_3}(s)+6H_2O(l)$
5.	$6Fe(OH)_2(s)+O_2(g)\rightarrow 2\mathbf{Fe_3O_4}(s)+6H_2O(l)$
6.	$Fe(s)+H_2SO_4(aq)\rightarrow \mathbf{FeSO_4}(aq)+H_2(g)$
7.	$2Fe(s)+3H_2SO_4(aq)\rightarrow \mathbf{Fe_2(SO_4)_3}(aq)+3H_2(g)$
8.	$Fe(s)+2HCl(aq)\rightarrow \mathbf{FeCl_2}(aq)+H_2(g)$
9.	$Fe(s)+6HCl(aq)\rightarrow 2\mathbf{FeCl_3}(aq)+3H_2(g)$
10.	$Fe(s)+Cl_2(g)\rightarrow \mathbf{FeCl_2}(s)$
11.	$FeS(s)+2HCl(aq)\rightarrow \mathbf{FeCl_2}(aq)+H_2S(g)$
12.	$2Fe(s)+3Cl_2(g)\rightarrow 2\mathbf{FeCl_3}(s)$
13.	$2FeCl_2(aq)+Cl_2(g)\rightarrow 2\mathbf{FeCl}_3(aq)$
14.	$Fe(s)+2FeCl_3(aq)\rightarrow 3\mathbf{FeCl_2}(aq)$
15.	$3Fe(s)+8H_2SO_4(aq)\rightarrow 3\mathbf{FeS}(s)+8H_2O(l)+8SO_2(g)$

In the corrosion process of iron (Fe) with oxygen (O_2) and water (H_2O), multiple compounds such as FeO, Fe_2O_3, Fe_3O_4, and $Fe(OH)_3$ are formed, with their specific types influenced by the solution's pH and oxygen concentration. The presence of sulfate and chloride ions in Puspiptek water further contributes to the formation of iron chloride and iron sulfate products, as evidenced by reactions (1)–(15) in Table 3. These include $FeSO_4(aq)$, $Fe_2(SO_4)_3(aq)$, and FeS(s), along with $FeCl_2(s)$ and $FeCl_3(aq)$, particularly under higher concentrations of chloride ions.

The formation of these corrosion products, including the ferrous and ferric sulfates from the interaction of iron with sulfuric acid in aqueous solutions, is driven by ongoing reactions among free ions, especially in environments rich in chloride, sulfate, and oxygen ions. These ions, as indicated in Table 1, are crucial to the corrosion mechanism, as they become confined within the metal grain lattice gaps and react with metal atoms, leading to pitting corrosion. This process is marked by the significant growth of pits in carbon steel,

particularly where specific elements like chlorine accumulate in crevices under stagnant flow conditions. The continuous attack of free ions on the metal surface and the formed corrosion products results in the persistent formation of new compounds. Observing these processes was challenging due to the ongoing nature of pitting corrosion over the 4-year immersion period.

Conclusions

A comprehensive scientific investigation was conducted to examine the corrosion behavior of carbon steel when exposed to PUSPIPTEK tap water over a four-year period. For this purpose, disc-shaped coupons of carbon steel and stainless steel 304 were employed to study various corrosion mechanisms in detail. The experimental findings indicate that the levels of sulfate and calcium ions in the water remained within the safe limits prescribed for industrial water systems. However, the concentration of chloride ions and the overall water hardness exceeded the permissible thresholds, thereby posing a potential risk for corrosion. The pH and electrical conductivity of the water were found to be within acceptable ranges, which is typically conducive to minimizing corrosive activity. However, despite these favorable conditions, the corrosion rate for carbon steel was measured at $1.19 \cdot 10^{-4}$ m per year, which is indicative of a significant degree of corrosion. Visual inspections of the coupons revealed extensive formation of corrosion products. Further, microscopic analysis of the corroded surfaces identified distinct patterns of surface degradation, which were indicative of the ongoing corrosive processes. X-Ray Diffraction (XRD) analysis was utilized to confirm the formation of corrosion-related compounds. This finding is a clear indication of active corrosion processes. A notable observation was that prolonged immersion in the tap water led to significant alterations in the metal surface structure, particularly at the grain boundaries. This alteration is a precursor to pitting corrosion, which was observed predominantly in crevices and areas forming galvanic circuits. The uniform corrosion observed in the coupon circuit was severe, suggesting a high rate of material degradation. In conclusion, the results of this study strongly advocate for the implementation of corrosion inhibitors in the secondary cooling water systems of the Research Reactor (RSG GAS) to mitigate further corrosion-related damage. The use of such inhibitors would be a proactive measure to extend the life of the system components and ensure safe and efficient operation.

Acknowledgement

The author would like to extend heartfelt thanks to the National Research and Innovation Agency (BRIN), the Research Center for Nuclear Reactor Technology (PRTRN), the Nuclear Technology Research Organization (ORTN), and Riset Inovasi Indonesia Maju (RIIM) for their generous financial support. This funding was instrumental in facilitating the successful completion of this research.

Contributorship

In this research, each author contributed equally and significantly to a well-structured process, encompassing the collaborative design of experimental samples, meticulous execution of experiments, and rigorous data collection. Analytical methods were carefully chosen for precise data interpretation, aligning the findings with our research objectives and existing literature. The collective effort in drafting, reviewing, and refining the manuscript ensured a clear, academically rigorous presentation of our results, underlining the study's reliability and scholarly merit.

References

1. S. Setiawati, H. Alikodra, B. Pramudya and A.H. Dharmawan, Model of Water, Energy and Waste Management for Development of Eco-Innovation Park ; A Case Study of Center for Research of Science and Technology "PUSPIPTEK," South Tangerang City, Indonesia, *World Technopolis Rev*., 2014, **3**, no. 2, 89–96. doi: 10.7165/wtr2014.3.2.89
2. G.R. Sunaryo, D.L. Lestari and Sriyono, Water Chemistry Surveillance for Multi Purpose Reactor 30 MW GA Siwabessy, Indonesia, *Proc. Int. Conf. Res. React. Safe Manag. Eff*., IAEA-CN--156, 2007, S56.
3. D. Wang, M.A. Mueses, J.A.C. Márquez, F. Machuca-Martínez, I. Grčić, R.P.M. Moreira and G. Li Puma, Engineering and modeling perspectives on photocatalytic reactors for water treatment, *Water Res*., 2021, **202**, 117421. doi: 10.1016/j.watres.2021.117421
4. S.M. Hosseini Pooya, M. Hosseinipanah and R. Adeli, Determination of urgent protective action zone in Tehran research reactors-associated accidents, *Nucl. Eng. Des*., 2021, **381**, 111356. doi: 10.1016/j.nucengdes.2021.111356
5. E. Boustani and S. Khakshournia, A liquid injection based Second Shutdown System for a typical material testing research reactor, *Ann. Nucl. Energy*, 2018, **115**, 487–493. doi: 10.1016/j.anucene.2018.01.047
6. I. Ahmed, E. Zio and G. Heo, Risk-informed approach to the safety improvement of the reactor protection system of the AGN-201K research reactor, *Nucl. Eng. Technol*., 2020, **52**, no. 4, 764–775. doi: 10.1016/j.net.2019.09.015
7. M. Jobst, P. Wilhelm, Y. Kozmenkov and S. Kliem, Severe accident management measures for a generic German PWR. Part II: Small-break loss-of-coolant accident, *Ann. Nucl. Energy*, 2018, **122**, 280–296. doi: 10.1016/j.anucene.2018.08.017
8. P. Pla, F. Reventos, M. Martin Ramos, I. Sol and M. Strucic, Simulation of steam generator plugging tubes in a PWR to analyze the operating impact, *Nucl. Eng. Des*., 2016, **305**, 132–145. doi: 10.1016/j.nucengdes.2016.05.002
9. J.I. Malik, N.M. Mirza and S.M. Mirza, Simulation of corrosion product activity in extended operating cycles of PWRs under flow rate transient and nonlinearly rising corrosion rates coupled with pH effects, *Nucl. Eng. Des*., 2012, **249**, 388–399. doi: 10.1016/j.nucengdes.2012.04.013

10. P.M. Udiyani, S. Kuntjoro, G.R. Sunaryo and H. Susiati, Atmospheric dispersion analysis for expected radiation dose due to normal operation of RSG-GAS and RDE reactors, *At. Indones*., 2018, **44**, no. 3. doi: 10.17146/aij.2018.878
11. Y.E. Yulianto and M. Imron, Manajemen Pengoperasian Reaktor RSG-GAS, *Pros. Semin. Nas. Teknol. Dan Apl. Reakt. Nukl. PRSG*., 2013, 15–23.
12. G.R. Sunaryo, R. Kusumastuti and Sriyono, Corrosion surveillance program for tank, fuel cladding and supporting structure of 30 MW Indonesian RSG GAS research reactor, *Kerntechnik*, 2021, **86**, 236–243. doi: 10.1515/kern-2020-0083
13. L. Zhang, W. Zhong, J. Yang, T. Gu, X. Xiao and M. Lu, Effects of temperature and partial pressure on H_2S–CO_2 corrosion of pipeline steel in sour conditions, *Int. Corros. Conf. Ser*., 2011.
14. A. Hernndez-Espejel, M.A. DomÌnguez-Crespo, R. Cabrera-Sierra, RodrÌguez-Meneses and E.M. Arce-Estrada, Investigations of corrosion films formed on API-X52 pipeline steel in acid sour media, *Corros. Sci*., 2010, **52**, no. 7, 2258–2267. doi: 10.1016/j.corsci.2010.04.003
15. J. Huang, D. Lister, S. Uchida and L. Liu, The corrosion of aluminium alloy and release of intermetallic particles in nuclear reactor emergency core coolant: Implications for clogging of sump strainers, *Nucl. Eng. Technol*., 2019, **51**, no. 5, 1345–1354. doi: 10.1016/j.net.2019.02.012
16. M.X. Milagre, U. Donatus, R.M.P. Silva, A.M. Betancor-Abreu, O.M.P. Ramirez, C.S.C. Machado, J.V.S. Araujo, R.M. Souto and I. Costa, Galvanic coupling effects on the corrosion behavior of the 6061 aluminum alloy used in research nuclear reactors, *J. Nucl. Mater*., 2020, **541**, 152440. doi: 10.1016/j.jnucmat.2020.152440
17. Z. Zhu, N. Tajallipour, P.J. Teevens, H. Xue and F.Y.F. Cheng, A mechanistic model for predicting localized-pitting corrosion in a brine water-CO_2 system, *Int. Corros. Conf. Ser*., 2011.
18. D.J.D. Garbe, D.K. Knierim, M.J. Acuna and M.K.C. Deokar, Modelling pitting corrosion in a CO_2 system containing bacteria, *Corrosion NACE*, Pap. no. 545, New Orleans, LA, Int., 2008.
19. G. Schmitt and S. Feinen, Effect of anions and cations on the pit initiation in CO_2 corrosion of iron and steel, *Corrosion NACE*, Pap. no. 1, Orlando, FL, 2000.
20. R.E. Melchers, Pitting corrosion of mild steel in marine immersion environment – Part 1: Maximum pit depth, *Corrosion*, 2004, **60**, no. 9, 824–836. doi: 10.5006/1.3287863
21. T. Subba Rao and S. Bera, Protective layer dissolution by chlorine and corrosion of aluminum brass condenser tubes of a nuclear power plant, *Eng. Failure Anal*., 2021, **123**, 105307. doi: 10.1016/j.engfailanal.2021.105307
22. M. Slobodyan, High-energy surface processing of zirconium alloys for fuel claddings of water-cooled nuclear reactors, *Nucl. Eng. Des*., 2021, **382**, 111364. doi: 10.1016/j.nucengdes.2021.111364

23. P. Suganya, G. Swaminathan, B. Anoop, G.V.R.R.S.G. Siva Prasad and J. Nagarajan, Assessing the factors affecting the water chemistry parameters in the auxiliary water system of a nuclear power plant, *SN Appl. Sci*., 2020, **2**, no. 1889, 1–13. doi: 10.1007/s42452-020-03693-z
24. *Corrosion of Research Reactor Aluminum Clad Spent Fuel in Water*, IAEA Library Cataloguing in Publication Data, 2010, 209.
25. G.R. Sunaryo, H. Sander and D.S. Wisnubroto, Water Chemistry Management toward Corrosion for Secondary Cooling Piping of Multi Purpose Reactor GA Siwabessy Indonesia, *Int. J. Eng. Res. Sci. Technol*., 2017, **3**, no. 6, 56–61. doi: 10.25125/engineering-journal-IJOER-JUN-2017-9
26. G.R. Sunaryo, Corrosion Management For Secondary Cooling Piping Of Multi Purpose Reactor 30 MW GA Siwabessy Indonesia, *RRFM Eur. Res. React. Conf*., 2012.
27. G.R. Sunaryo, Surveillance Management for Secondary Water Cooling Quality of RSG GAS, *J. Sains Dan Teknol. Nukl. Indones*., 2017, **18**, no. 7. doi: 10.17146/jstni.2017.18.1.3214
28. G.R. Sunaryo and Sriyono, Spent Fuel Storage Corrosion Management, *Int. Conf. Res. React. Safe Manag. Eff. Util*., 2011, 1–7.
29. G. Sunaryo, Aplikasi Program Corrosion Surveillance untuk Kolam Penyimpan Reaktor RSG-GAS, *Semin. TKPFN Surabaya Surabaya*, 2010, 158–164.
30. P.R. Roberge, *Handbook of Corrosion Engineering*, 2012. doi: 10.5860/choice.37-5122
31. V. Raja and B.S. Padekar, Role of chlorides on pitting and hydrogen embrittlement of Mg–Mn wrought alloy, *Corros. Sci*., 2013, **75**, 176–183.
32. J. Bhandari, F. Khan, R. Abbassi, V. Garaniya and R. Ojeda, Modelling of pitting corrosion in marine offshore steel structures – A technical review, *J. Loss Prev. Process Ind*., 2015, **37**, 39–62. doi: 10.1016/j.jlp.2015.06.008
33. K.A. Lichti, M. Ko and L. Wallis, Galvanic corrosion study of carbon steel to arsenic and antimoby couples, *Geothermics*, 2015, **58**, 15–21. doi: 10.1016/j.geothermics.2015.07.006
34. F. Febrianto, G.R. Sunaryo and S.L. Butarbutar, Analisis Laju Korosi dengan Penambahan Inhibitor Korosi pada Pipa Sekunder Reaktor RSG GAS, *Semin. Nas. VI SDM Teknol. Nukl. Yogyakarta*, 2010, 615–618.
35. H.H. Revie and R Winston, *Uhlig, Corrosion and corrosion control an introduction to corrosion science and engineering*, 2008.
36. D.A. Jones, *Principles and prevention of corrosion, second edition*, 1996.
37. D.E. Jensen and G.A. Jones, Iron compounds in flames. Relative stabilities of Fe, FeO, FeOH and $Fe(OH)_2$, *J. Chem. Soc., Faraday Trans. 1*., 1973, **69**, 1448–1454.

♦ ♦ ♦